



# SOLAR OBLIQUITY INDUCED BY PLANET NINE

ELIZABETH BAILEY, KONSTANTIN BATYGIN, AND MICHAEL E. BROWN

Division of Geological and Planetary Sciences, California Institute of Technology, Pasadena, CA 91125, USA; [ebailey@gps.caltech.edu](mailto:ebailey@gps.caltech.edu)

Received 2016 June 24; revised 2016 August 12; accepted 2016 August 23; published 2016 October 21

## ABSTRACT

The six-degree obliquity of the Sun suggests that either an asymmetry was present in the solar system’s formation environment, or an external torque has misaligned the angular momentum vectors of the Sun and the planets. However, the exact origin of this obliquity remains an open question. Batygin & Brown have recently shown that the physical alignment of distant Kuiper Belt orbits can be explained by a 5–20  $m_{\oplus}$  planet on a distant, eccentric, and inclined orbit, with an approximate perihelion distance of  $\sim 250$  au. Using an analytic model for secular interactions between Planet Nine and the remaining giant planets, here, we show that a planet with similar parameters can naturally generate the observed obliquity as well as the specific pole position of the Sun’s spin axis, from a nearly aligned initial state. Thus, Planet Nine offers a testable explanation for the otherwise mysterious spin–orbit misalignment of the solar system.

*Key words:* planets and satellites: dynamical evolution and stability

## 1. INTRODUCTION

The axis of rotation of the Sun is offset by six degrees from the invariable plane of the solar system (Souami & Souchay 2012). In contrast, planetary orbits have an rms inclination slightly smaller than one degree,<sup>1</sup> rendering the solar obliquity a considerable outlier. The origin of this misalignment between the Sun’s rotation axis and the angular momentum vector of the solar system has been recognized as a long-standing question (Kuiper 1951; Tremaine 1991; Heller 1993), and remains elusive to this day.

With the advent of extensive exoplanetary observations, it has become apparent that significant spin–orbit misalignments are common, at least among transiting systems for which the stellar obliquity can be determined using the Rossiter–McLaughlin effect (McLaughlin 1924; Rossiter 1924). Numerous such observations of planetary systems hosting hot Jupiters have revealed spin–orbit misalignments spanning tens of degrees (Hébrard et al. 2008; Winn et al. 2010; Albrecht et al. 2012), even including observations of retrograde planets (Narita et al. 2009; Winn et al. 2009, 2011; Bayliss et al. 2010). Thus, when viewed in the extrasolar context, the solar system seems hardly misaligned. However, within the framework of the nebular hypothesis, the expectation for the offset between the angular momentum vectors of the planets and Sun is to be negligible, unless a specific physical mechanism induces a misalignment. Furthermore, the significance of the solar obliquity is supported by the contrasting relative coplanarity of the planets.

Because there is no directly observed stellar companion to the Sun (or any other known gravitational influence capable of providing an external torque on the solar system sufficient to produce a six-degree misalignment over its multi-billion-year lifetime Heller 1993), virtually all explanations for the solar obliquity thus far have invoked mechanisms inherent to the nebular stage of evolution. In particular, interactions between the magnetosphere of a young star and its protostellar disk can potentially lead to a wide range of stellar obliquities, while

leaving the coplanarity of the tilted disk intact (Lai et al. 2011). However, another possible mechanism by which the solar obliquity could be attained in the absence of external torque is an initial asymmetry in the mass distribution of the protostellar core. Accordingly, asymmetric infall of turbulent protosolar material has been proposed as a mechanism for the Sun to have acquired an axial tilt upon formation (Bate et al. 2010; Fielding et al. 2015). However, the capacity of these mechanisms to overcome the re-aligning effects of accretion, as well as gravitational and magnetic coupling, remains an open question (Lai et al. 2011; Spalding & Batygin 2014, 2015).

In principle, solar obliquity could have been excited through a temporary, extrinsic gravitational torque early in the solar system’s lifetime. That is, an encounter with a passing star or molecular cloud could have tilted the disk or planets with respect to the Sun (Heller 1993; Adams 2010). Alternatively, the Sun may have had a primordial stellar companion, capable of early star-disk misalignment (Batygin 2012; Spalding & Batygin 2014; Lai 2014). To this end, ALMA observations of misaligned disks in stellar binaries (Jensen & Akeson 2014; Williams et al. 2014) have provided evidence for the feasibility of this effect. Although individually sensible, a general qualitative drawback of all of the above mechanisms is that they are only testable when applied to the extrasolar population of planets, and it is difficult to discern which (if any) of the aforementioned processes operated in our solar system.

Recently, Batygin & Brown (2016) determined that the spatial clustering of the orbits of Kuiper Belt objects with semimajor axes of  $a \gtrsim 250$  au can be understood if the solar system hosts an additional  $m_9 = 5\text{--}20 m_{\oplus}$  planet on a distant, eccentric orbit. Here, we refer to this object as Planet Nine. The orbital parameters of this planet reside somewhere along a swath of parameter space spanning hundreds of astronomical units in semimajor axis, significant eccentricity, and tens of degrees of inclination, with a perihelion distance of roughly  $q_9 \sim 250$  au (Brown & Batygin 2016). In this work, we explore the possibility that this distant, planetary-mass body is fully or partially responsible for the peculiar spin axis of the Sun.

<sup>1</sup> An exception to the observed orbital coplanarity of the planets is Mercury, whose inclination is subject to chaotic evolution (Laskar 1994; Batygin et al. 2015)

Induction of solar obliquity of some magnitude is an inescapable consequence of the existence of Planet Nine. That is, the effect of a distant perturber residing on an inclined orbit is to exert a mean-field torque on the remaining planets of the solar system, over a timespan of  $\sim 4.5$  Gyr. In this manner, the gravitational influence of Planet Nine induces precession of the angular momentum vectors of the Sun and planets about the total angular momentum vector of the solar system. Provided that angular momentum exchange between the solar spin axis and the planetary orbits occurs on a much longer timescale, this process leads to a differential misalignment of the Sun and planets. Below, we quantify this mechanism with an eye toward explaining the tilt of the solar spin axis with respect to the orbital angular momentum vector of the planets.

The paper is organized as follows. Section (2) describes the dynamical model. We report our findings in Section (3). We conclude and discuss our results in Section (4). Throughout the manuscript, we adopt the following notation. Similarly named quantities (e.g.,  $a$ ,  $e$ ,  $i$ ) related to Planet Nine are denoted with a subscript “9,” whereas those corresponding to the Sun’s angular momentum vector in the inertial frame are denoted with a tilde. Solar quantities measured with respect to the solar system’s invariable plane are given the subscript  $\odot$ .

## 2. DYNAMICAL MODEL

To model the long-term angular momentum exchange between the known giant planets and Planet Nine, we employ secular perturbation theory. Within the framework of this approach, Keplerian motion is averaged out, yielding semi-major axes that are frozen in time. Correspondingly, the standard  $N$ -planet problem is replaced with a picture in which  $N$  massive wires (whose line densities are inversely proportional to the instantaneous orbital velocities) interact gravitationally (Murray & Dermott 1999). Provided that no low-order commensurabilities exist among the planets, this method is well known to reproduce the correct dynamical evolution on timescales that greatly exceed the orbital period (Mardling 2007; Li et al. 2014).

In choosing which flavor of secular theory to use, we must identify small parameters inherent to the problem. Constraints based upon the critical semimajor axis beyond which orbital alignment ensues in the distant Kuiper Belt suggest that Planet Nine has an approximate perihelion distance of  $q_9 \sim 250$  au and an appreciable eccentricity  $e_9 \gtrsim 0.3$  (Batygin & Brown 2016; Brown & Batygin 2016). Therefore, the semimajor axis ratio ( $a/a_9$ ) can safely be assumed to be small. Additionally, because solar obliquity itself is small and the orbits of the giant planets are nearly circular, here we take  $e = 0$  and  $\sin(i) \ll 1$ . Under these approximations, we can expand the averaged planet–planet gravitational potential in small powers of  $(a/a_9)$ , and only retain terms of leading order in  $\sin(i)$ .

In principle, we could self-consistently compute the interactions among all of the planets, including Planet Nine. However, because the fundamental secular frequencies that characterize angular momentum exchange among the known giant planets are much higher than that associated with Planet Nine, the adiabatic principle (Henrard 1982; Neishtadt 1984) ensures that Jupiter, Saturn, Uranus, and Neptune will remain coplanar with each-other throughout the evolutionary sequence (see, e.g., Batygin et al. 2011a; Batygin 2012 for a related discussion on

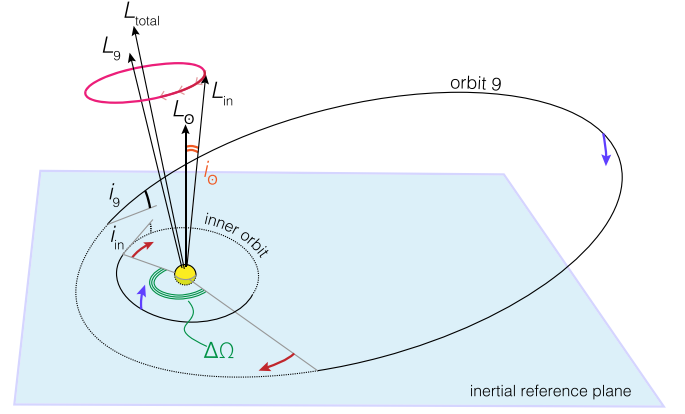


**Figure 1.** Geometric setup of the dynamical model. The orbits of the planets are treated as gravitationally interacting rings. All planets except Planet Nine are assumed to have circular, mutually coplanar orbits, and are represented as a single inner massive wire. The Sun is shown as a yellow sphere, and elements are not to scale. Black, gray, and dotted lines are respectively above, on, and below the inertial reference plane. The pink arrows demonstrate the precession direction of the angular momentum vector of the inner orbit,  $L_{\text{in}}$ , around the total angular momentum vector of the solar system  $L_{\text{total}}$ . Red and blue arrows represent the differential change in longitudes of ascending node of the orbits and inclination, respectively. Although not shown in the figure, the tilting of the oblate Sun is modeled as the tilting of an inner test ring. Over the course of 4.5 billion years, differential precession of the orbits induces a several-degree solar obliquity with respect to the final plane of the planets.

perturbed self-gravitating disks). As a result, rather than modeling four massive rings individually, we may collectively replace them with a single circular wire having semimajor axis  $a$  and mass  $m$ , and possessing equivalent total angular momentum and moment of inertia

$$\begin{aligned} m \sqrt{a} &= \sum_j m_j \sqrt{a_j} \\ m a^2 &= \sum_j m_j a_j^2, \end{aligned} \quad (1)$$

where the index  $j$  runs over all planets. The geometric setup of the problem is shown in Figure (1).

To quadrupole order, the secular Hamiltonian governing the evolution of two interacting wires is (Kaula 1962; Mardling 2010)

$$\begin{aligned} \mathcal{H} = \frac{\mathcal{G} m m_9}{4 a_9} \left( \frac{a}{a_9} \right)^2 \frac{1}{\varepsilon_9^3} &\left[ \frac{1}{4} (3 \cos^2(i) - 1) (3 \cos^2(i_9) - 1) \right. \\ &\left. + \frac{3}{4} \sin(2i) \sin(2i_9) \cos(\Omega - \Omega_9) \right], \end{aligned} \quad (2)$$

where  $\Omega$  is the longitude of the ascending node and  $\varepsilon_9 = \sqrt{1 - e_9^2}$ . Note that while the eccentricities and inclinations of the known giant planets are assumed to be small, no limit is placed on the orbital parameters of Planet Nine. Moreover, at this level of expansion, the planetary eccentricities remain unmodulated, consistent with the numerical simulations of Batygin & Brown (2016) and Brown & Batygin (2016), where the giant planets and Planet Nine are observed to behave in a decoupled manner.

Although readily interpretable, Keplerian orbital elements do not constitute a canonically conjugated set of coordinates. Therefore, to proceed, we introduce Poincaré action-angle coordinates:

$$\begin{aligned}\Gamma &= m\sqrt{\mathcal{G}M_\odot a} \\ \Gamma_9 &= m_9\sqrt{\mathcal{G}M_\odot a_9} \varepsilon_9 \\ Z &= \Gamma(1 - \cos(i)) \quad z = -\Omega \\ Z_9 &= \Gamma_9(1 - \cos(i_9)) \quad z = -\Omega_9.\end{aligned}\quad (3)$$

Generally, the action  $Z$  represents the deficit of angular momentum along the  $\hat{k}$ -axis, and to leading order,  $i \approx \sqrt{2Z/\Gamma}$ . Accordingly, dropping higher-order corrections in  $i$ , expression (2) takes the form

$$\begin{aligned}\mathcal{H} &= \frac{\mathcal{G} m m_9}{4} \left(\frac{a}{a_9}\right)^2 \frac{1}{\varepsilon_9^3} \left[ \frac{1}{4} \left( 2 - \frac{6Z}{\Gamma} \right) \left( 3 \left( 1 - \frac{Z_9}{\Gamma_9} \right)^2 - 1 \right) \right. \\ &\quad \left. + 3 \left( 1 - \frac{Z_9}{\Gamma_9} \right) \sqrt{1 - \frac{Z_9}{2\Gamma_9}} \sqrt{\frac{2Z}{\Gamma} \frac{2Z_9}{\Gamma_9}} \cos(z - z_9) \right].\end{aligned}\quad (4)$$

Application of Hamilton's equations to this expression yields the equations of motion governing the evolution of the two-ring system. However, we note that action-angle variables (3) are singular at the origin, so an additional, trivial change to Cartesian counterparts of Poincaré coordinates is required to formulate a practically useful set of equations (Morbidelli 2002). This transformation is shown explicitly in the Appendix.

To complete the specification of the problem, we also consider the torque exerted on the Sun's spin axis by a tilting solar system. Because the Sun's angular momentum budget is negligible compared to that of the planets, its back-reaction on the orbits can be safely ignored. Then, the dynamical evolution of its angular momentum vector can be treated within the same framework of secular theory, by considering the response of a test ring with the semimajor axis (Spalding & Batygin 2014, 2015):

$$\tilde{a} = \left[ \frac{16 \omega^2 k_2^2 R^6}{9 I^2 \mathcal{G} M_\odot} \right]^{1/3}, \quad (5)$$

where  $\omega$  is the rotation frequency,  $k_2$  is the Love number,  $R$  is the solar radius, and  $I$  is the moment of inertia.

Because we are primarily concerned with main-sequence evolution, here we adopt  $R = R_\odot$  and model the interior structure of the Sun as a  $n = 3$  polytrope, appropriate for a fully radiative body (Chandrasekhar 1939). Corresponding values of moment of inertia and Love number are  $I = 0.08$  and  $k_2 = 0.01$  respectively (Batygin & Adams 2013). The initial rotation frequency is assumed to correspond to a period of  $2\pi/\omega = 10$  days and is taken to decrease as  $\omega \propto 1/\sqrt{I}$ , in accordance with the Skumanich relation (Gallet & Bouvier 2013).

Defining scaled actions  $\tilde{\Gamma} = \sqrt{\mathcal{G}M_\odot} \tilde{a}$  and  $\tilde{Z} = \tilde{\Gamma}(1 - \cos(\tilde{i}))$  and scaling the Hamiltonian itself in the same way, we can write down a Hamiltonian that is essentially analogous to Equation (4), which governs the long-term spin

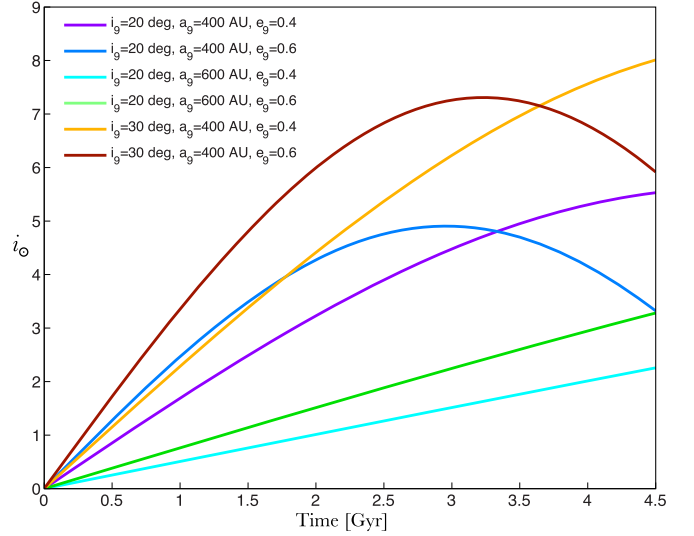


**Figure 2.** Time evolution of the solar obliquity  $i_\odot$  in the frame of the solar system, starting with an aligned configuration of the solar system, and a  $10m_\oplus$  Planet Nine with starting parameters in the example range  $a_9 \in [400, 600]$  au,  $e_9 \in [0.4, 0.6]$ , and  $i_9 \in [20, 30]$  deg.

axis evolution of the Sun:

$$\tilde{\mathcal{H}} = \sum_j \left( \frac{\mathcal{G} m_j}{4 a_j^3} \right) \tilde{a}^2 \left[ \frac{3\tilde{Z}}{\tilde{\Gamma}} + \frac{3}{4} \sqrt{\frac{2\tilde{Z}}{\tilde{\Gamma}}} \frac{2\tilde{Z}}{\tilde{\Gamma}} \cos(\tilde{z} - z) \right]. \quad (6)$$

Note that contrary to Equation (4), here we have assumed small inclinations for both the solar spin axis and the planetary orbits. This assumption transforms the Hamiltonian into a form equivalent to the Lagrange–Laplace theory, where the interaction coefficients have been expanded as hypergeometric series, to leading order in the semimajor axis ratio (Murray & Dermott 1999). Although not particularly significant in magnitude, we follow the evolution of the solar spin axis for completeness.

Quantitatively speaking, there are two primary sources of uncertainty in our model. The first is the integration timescale. Although the origin of Planet Nine is not well understood, its early evolution was likely affected by the presence of the solar system's birth cluster (Izidoro et al. 2015; Li & Adams 2016), meaning that Planet Nine probably attained its final orbit within the first  $\sim 100$  Myr of the solar system's lifetime. Although we recognize the  $\sim 2\%$  error associated with this ambiguity, we adopt an integration timescale of 4.5 Gyr for definitiveness.

A second source of error stems from the fact that the solar system's orbital architecture almost certainly underwent an instability-driven transformation sometime early in its history (Tsiganis et al. 2005; Nesvorný & Morbidelli 2012). Although the timing of the onset of instability remains an open question (Levison et al. 2011; Kaib & Chambers 2016), we recognize that the failure of our model to reflect this change in  $a$  and  $m$  (through Equation (1)) introduces a small degree of inaccuracy into our calculations. Nevertheless, it is unlikely that these detailed complications constitute a significant drawback to our results.



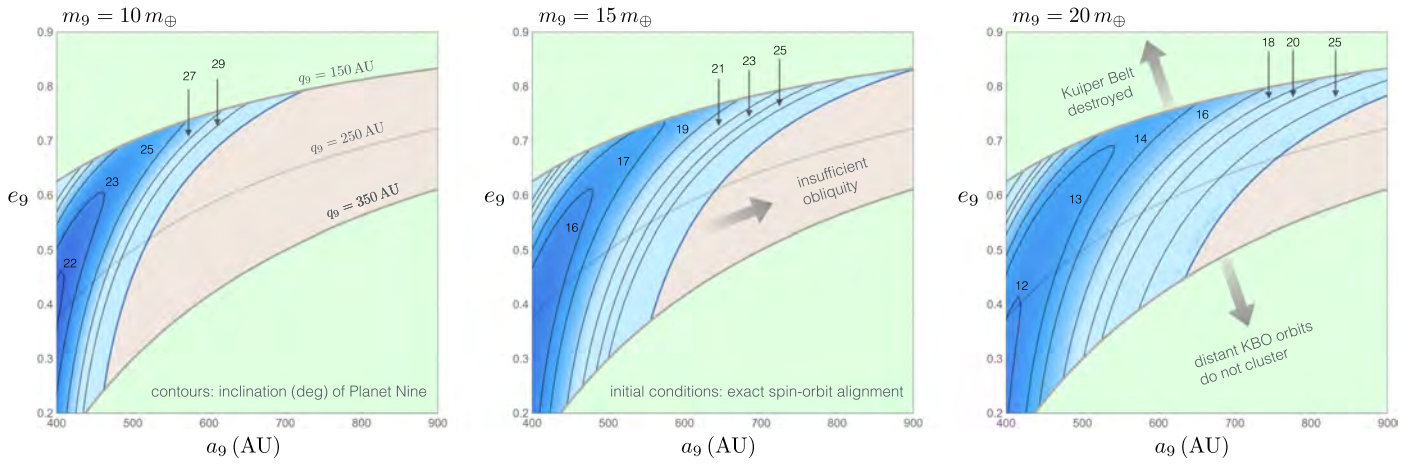


**Figure 3.** Parameters of Planet Nine required to excite a spin–orbit misalignment of  $i_{\odot} = 6^{\circ}$  over the lifetime of the solar system, from an initially aligned state. Contours in  $a_9$ – $e_9$  space denote  $i_9$ , required to match the present-day solar obliquity. Contour labels are quoted in degrees. The left, middle, and right panels correspond to  $m_9 = 10$ , 15, and  $20 m_{\oplus}$  respectively. Due to independent constraints stemming from the dynamical state of the distant Kuiper Belt, only orbits that fall in the  $150 < q_9 < 350$  au range are considered. The portion of parameter space where a solar obliquity of  $i_{\odot} = 6^{\circ}$  cannot be attained are obscured with a light-brown shade.

### 3. RESULTS

As shown in Figure (2), the effect of Planet Nine is to induce a gradual differential precession of the Sun and the solar system’s invariable plane,<sup>2</sup> resulting in a solar obliquity of several degrees over the lifetime of the solar system. The Sun’s present-day inclination with respect to the solar system’s invariable plane (Souami & Souchay 2012) is almost exactly  $i_{\odot} = 6^{\circ}$ . Using this number as a constraint, we have calculated the possible combinations of  $a_9$ ,  $e_9$ , and  $i_9$  for a given  $m_9$ , that yield the correct spin–orbit misalignment after 4.5 Gyr of evolution. For this set of calculations, we adopted an initial condition in which the Sun’s spin axis and the solar system’s total angular momentum vector were aligned.

The results are shown in Figure (3). For three choices of  $m_9 = 10$ , 15, and  $20 m_{\oplus}$ , the figure depicts contours of the required  $i_9$  in  $a_9$  –  $e_9$  space. Because Planet Nine’s perihelion distance is approximately  $q_9 \sim 250$  au, we have only considered orbital configurations with  $150 < q_9 < 350$  au. Moreover, within the considered locus of solutions, we neglect the region of parameter space where the required solar obliquity cannot be achieved within the lifetime of the solar system. This section of the graph is shown with a light-brown shade in Figure (3).

For the considered range of  $m_9$ ,  $a_9$ , and  $e_9$ , characteristic inclinations of  $i_9 \sim 15^{\circ}$ – $30^{\circ}$  are required to produce the observed spin–orbit misalignment. This compares favorably with the results of Brown & Batygin (2016), where a similar inclination range for Planet Nine is obtained from entirely different grounds. However, we note that the constraints on  $a_9$  and  $e_9$  seen in Figure (3) are somewhat more restrictive than those in previous works. In particular, the illustrative  $m_9 = 10 m_{\oplus}$ ,  $a_9 = 700$  au,  $e_9 = 0.6$  perturber considered by Batygin & Brown (2016), as well as virtually all of the “high-probability” orbits computed by Brown & Batygin (2016) fall short of exciting  $6^{\circ}$  of obliquity from a strictly coplanar initial configuration. Instead, slightly smaller spin–orbit misalignments of  $i_{\odot} \sim 3^{\circ}$ – $5^{\circ}$  are typically obtained. At the same time,

we note that the lower bound on the semimajor axis of Planet Nine quoted in Brown & Batygin (2016) is based primarily on the comparatively low perihelia of the unaligned objects, rather than the alignment of distant Kuiper Belt objects, constituting a weaker constraint.

An equally important quantity as the solar obliquity itself, is the solar longitude of the ascending node<sup>3</sup>  $\Omega_{\odot} \simeq 68^{\circ}$ . This quantity represents the azimuthal orientation of the spin axis and informs the direction of angular momentum transfer within the system. While the angle itself is measured from an arbitrary reference point, the difference in longitudes of ascending node  $\Delta\Omega = \Omega_9 - \Omega_{\odot}$  is physically meaningful, and warrants examination.

Figure (4) shows contours of  $\Delta\Omega$  within the same parameter space as Figure (3). Evidently, the representative range of the relative longitude of ascending node is  $\Delta\Omega \sim -60^{\circ}$  to  $40^{\circ}$ , with the positive values coinciding with high eccentricities and low semimajor axes. Therefore, observational discovery of Planet Nine with a correspondent combination of parameters  $a_9$ ,  $e_9$ ,  $i_9$ , and  $\Delta\Omega$  depicted anywhere on an analog of Figures (3) and (4) constructed for the specific value of  $m_9$ , would constitute formidable evidence that Planet Nine is solely responsible for the peculiar spin axis of the Sun. On the contrary, a mismatch of these parameters relative to the expected values would imply that Planet Nine has merely modified the Sun’s spin axis by a significant amount.

Although  $\Omega_9$  is not known, Planet Nine’s orbit is theoretically inferred to reside in approximately the same plane as the distant Kuiper Belt objects, whose longitudes of ascending node cluster around  $\langle\Omega\rangle = 113^{\circ} \pm 13^{\circ}$  (Batygin & Brown 2016). Therefore, it is likely that  $\Omega_9 \simeq \langle\Omega\rangle$ , implying that  $\Delta\Omega \simeq 45^{\circ}$ . Furthermore, the simulation suite of Brown & Batygin (2016) approximately constrains Planet Nine’s longitude of the ascending node to the range of  $\Omega_9 \simeq 80^{\circ}$ – $120^{\circ}$ , yielding  $12^{\circ} < \Delta\Omega < 52^{\circ}$  as an expected range of solar spin axis orientations.

If we impose the aforementioned range of  $\Delta\Omega$  as a constraint on our calculations, Figure (4) suggests that  $a_9 \lesssim 500$  au and

<sup>2</sup> Although we refer to the instantaneous plane occupied by the wire with parameters  $a$  and  $m$  as the invariable plane, in our calculations, this plane is not actually invariable. Instead, it slowly precesses in the inertial frame.

<sup>3</sup> The quoted value is measured with respect to the invariable plane, rather than the ecliptic.



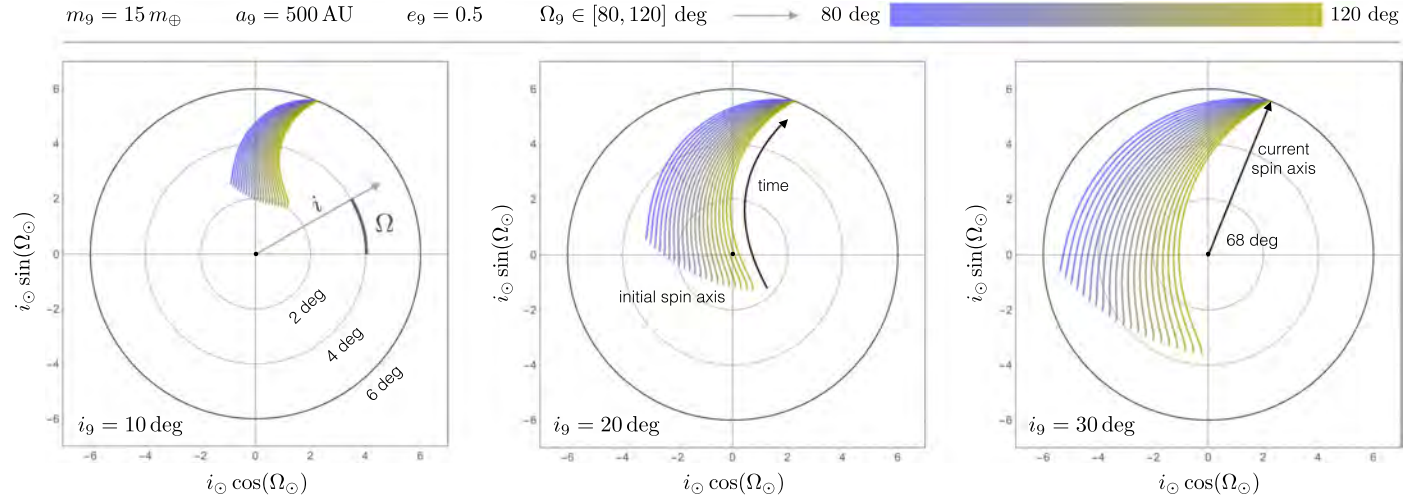


**Figure 5.** Illustrative evolution tracks of the solar spin axis, measured with respect to the instantaneous invariable plane. The graphs are shown in polar coordinates, where  $i_{\odot}$  and  $\Omega_{\odot}$  represent the radial and angular variables respectively. The integrations are initialized with the Sun’s present-day configuration ( $i_{\odot} = 6^{\circ}$ ,  $\Omega_{\odot} = 68^{\circ}$ ), and are performed backward in time. For Planet Nine, parameters of  $m_9 = 15 m_{\oplus}$ ,  $a_9 = 500$  au, and  $e_9 = 0.5$  are adopted throughout. Meanwhile, the left, middle, and right panels show results corresponding to  $i_9 = 10^{\circ}$ ,  $20^{\circ}$ , and  $30^{\circ}$  respectively. The present-day longitude of the ascending node of Planet Nine is assumed to lie in the range of  $80^{\circ} < \Omega_9 < 120^{\circ}$  and is represented by the color of the individual evolution tracks.

primordial solar obliquity within the emerging extrasolar trend of small spin–orbit misalignments in flat planetary systems (Morton & Winn 2014), and bring the computed value closer to the expectations of the nebular hypothesis. However, we note that, at present, the range of unconstrained parameters also allows for an evolutionary sequences in which Planet Nine’s contribution does not play a dominant role in exciting the solar obliquity.

Gomes et al. (2016) independently reached similar conclusions. The primary differences between the two studies arise from the specific choice of methodology and the preference of Gomes et al. (2016) to consider select inclinations of Planet Nine, which are significantly higher than the  $\sim 20^{\circ}$  inclination of the distant cluster of Kuiper Belt objects that first engendered the Planet Nine hypothesis (Batygin & Brown 2016).

The integrable nature of the calculations performed in this work imply that observational characterization of Planet Nine’s orbit will not only verify the expansion of the solar system’s planetary album, but will yield remarkable new insights into the state of the solar system, at the time of its formation. That is, if Planet Nine is discovered in a configuration that contradicts a strictly aligned initial condition of the solar spin axis and planetary angular momentum, calculations of the type performed herein can be used to deduce the true primordial obliquity of the Sun. In turn, this information can potentially constrain the mode of magnetospheric interactions between the young Sun and the solar nebula (Konigl 1991; Lai et al. 2011; Spalding & Batygin 2015), as well as place meaningful limits on the existence of a putative primordial stellar companion of the Sun (Batygin 2012; Xiang-Gruess & Papaloizou 2014).

Finally, this work provides not only a crude test of the likely parameters of Planet Nine, but also a test of the viability of the Planet Nine hypothesis. By definition, Planet Nine is hypothesized to be a planet having parameters sufficient to induce the observed orbital clustering of Kuiper Belt objects with semimajor axis  $a > 250$  au (Batygin & Brown 2016). According to this definition, Planet Nine must occupy a narrow

swath in  $a - e$  space such that  $q_9 \sim 250$  au, and its mass must reside in the approximate range  $m_9 = 5\text{--}20 m_{\oplus}$ . If Planet Nine were found to induce a solar obliquity significantly higher than the observed value, the Planet Nine hypothesis could be readily rejected. Instead, here we have demonstrated that, over the lifetime of the solar system, Planet Nine typically excites a solar obliquity that is similar to what is observed, giving additional credence to the Planet Nine hypothesis.

We are grateful to Chris Spalding and Roger Fu for useful discussions, and to the anonymous reviewer for insightful comments.

## APPENDIX

To octupole order in  $(a/a_9)$ , the full Hamiltonian governing the secular evolution of a hierarchical triple is (Kaula 1962; Mardling 2010)

$$\begin{aligned} \mathcal{H} = & -\frac{1}{4} \frac{\mathcal{G} \mu m_9}{a_9} \left( \frac{a}{a_9} \right)^2 \frac{1}{\varepsilon_9^3} \left[ \left( 1 + \frac{3}{2} e^2 \right) \frac{1}{4} (3 \cos(i) - 1) \right. \\ & \times (3 \cos(i_9) - 1) + \frac{15}{14} e^2 \sin^2(i) \cos(2\omega) \\ & + \frac{3}{4} \sin(2i) \sin(2i_9) \cos(\Omega - \Omega_9) \\ & \left. + \frac{3}{4} \sin^2(i) \sin^2(i_9) \cos(2\Omega - 2\Omega_9) \right], \end{aligned}$$

where elements without a subscript refer to the inner body, and elements with subscript 9 refer to the outer body, in this case, Planet Nine. Here  $\mu = (M_{\odot} m)/(M_{\odot} + m) \approx m$ , and  $\varepsilon_9$  is equal to  $\sqrt{1 - e_9^2}$ .

To attain integrability, we drop the Kozai harmonic because comparatively rapid perihelion precession of the known giant planets’ orbits ensures that libration of  $\omega$  is not possible (Batygin et al. 2011b). Because the eccentricities of the known



giant planets are small, we adopt  $e = 0$  for the inner orbit. Additionally, because the inclination of the inner orbit is presumed to be small throughout the evolutionary sequence, we neglect the higher-order  $\cos(2\Omega - 2\Omega_9)$  harmonic, because it is proportional to  $\sin^2(i) \ll \sin(2i) \ll 1$ .

Keeping in mind the trigonometric relationship  $\sin i = \sqrt{1 - \cos^2 i}$ , and adopting canonical Poincaré action-angle variables given by Equation (3), the Hamiltonian takes the approximate form

$$\begin{aligned} \mathcal{H} = & -\frac{1}{4} \frac{\mathcal{G} m m_9}{a_9} \left( \frac{a}{a_9} \right)^2 \frac{1}{\varepsilon^3} \left[ \frac{1}{4} \left( 3 \left( 1 - \frac{Z}{\Gamma} \right)^2 - 1 \right) \right. \\ & \times \left( 3 \left( 1 - \frac{Z_9}{\Gamma_9} \right)^2 - 1 \right) + \frac{3}{4} \left( 2 \left( 1 - \frac{Z}{\Gamma} \right) \right. \\ & \times \left. \sqrt{1 - \left( 1 - \frac{Z}{\Gamma} \right)^2} \right) \left( 2 \left( 1 - \frac{Z_9}{\Gamma_9} \right) \sqrt{1 - \left( 1 - \frac{Z_9}{\Gamma_9} \right)^2} \right) \\ & \left. \times \cos(z - z_9) \right]. \end{aligned}$$

Because the inner orbit has a small inclination, it is suitable to expand  $\mathcal{H}$  to leading order in  $Z$ . This yields the Hamiltonian given in Equation (4).

Since Hamiltonian (4) possesses only a single degree of freedom, the Arnold–Liouville theorem (Arnold 1963) ensures that by application of the Hamilton–Jacobi equation,  $\mathcal{H}$  can be cast into a form that only depends on the actions. Then, the entirety of the system’s dynamics is encapsulated in the linear advance of cyclic angles along contours defined by the constants of motion (Morbidelli 2002). Here, rather than carrying out this extra step, we take the more practically simple approach of numerically integrating the equations of motion, while keeping in mind that the resulting evolution is strictly regular.

The numerical evaluation of the system’s evolution can be robustly carried out after transforming the Hamiltonian to nonsingular Poincaré Cartesian coordinates

$$\begin{aligned} x &= \sqrt{2Z} \cos(z) & y &= \sqrt{2Z} \sin(z) \\ x_9 &= \sqrt{2Z_9} \cos(z_9) & y_9 &= \sqrt{2Z_9} \sin(z_9). \end{aligned}$$

Then, the truncated and expanded Hamiltonian (4) becomes

$$\begin{aligned} \mathcal{H} = & -\frac{1}{4} \frac{\mathcal{G} m m_9}{a_9} \left( \frac{a}{a_9} \right)^2 \frac{1}{\varepsilon_9^3} \left[ \frac{1}{4} \left( 2 - \frac{6}{\Gamma} \left( \frac{x^2 + y^2}{2} \right) \right) \right. \\ & \times \left( 3 \left( 1 - \frac{1}{\Gamma_9} \left( \frac{x_9^2 + y_9^2}{2} \right) \right)^2 - 1 \right) \\ & + 3 \left( 1 - \frac{1}{\Gamma_9} \left( \frac{x_9^2 + y_9^2}{2} \right) \right) \\ & \left. \times \sqrt{1 - \frac{1}{2\Gamma_9} \left( \frac{x_9^2 + y_9^2}{2} \right)} \sqrt{\frac{1}{\Gamma\Gamma_9}} (xx_9 + yy_9) \right]. \end{aligned}$$

Explicitly, Hamilton’s equations  $dx/dt = -\partial\mathcal{H}/\partial y$ ,  $dy/dt = \partial\mathcal{H}/\partial x$  take the form

$$\begin{aligned} \frac{dx}{dt} = & \frac{a^2 \mathcal{G} m m_9}{4 a_9^3 \varepsilon_9^3} \left( \frac{3y_9(2\Gamma_9 - x_9^2 - y_9^2)}{4\Gamma_9} \sqrt{\frac{4\Gamma_9 - x_9^2 - y_9^2}{\Gamma\Gamma_9^2}} \right. \\ & \left. + \frac{3y}{2\Gamma} \left( 1 - \frac{3(2\Gamma_9 - x_9^2 - y_9^2)^2}{4\Gamma_9^2} \right) \right) \\ \frac{\partial y}{\partial t} = & \frac{3 a^2 \mathcal{G} m m_9}{32 a_9^3 \Gamma \Gamma_9^2 \varepsilon_9^3} \\ & \times (2x_9 \sqrt{\Gamma(4\Gamma_9 - x_9^2 - y_9^2)} (x_9^2 + y_9^2 - 2\Gamma_9) \\ & + x(8\Gamma_9^2 + 3x_9^4 - 12\Gamma_9 y_9^2 + 3y_9^4 + 6x_9^2(y_9^2 - 2\Gamma_9))) \\ \frac{\partial x_9}{\partial t} = & \frac{3 a^2 \mathcal{G} m m_9}{16 a_9^3 \Gamma_9^2 \varepsilon_9^3} (-2y_9(xx_9 + yy_9) \\ & \times \sqrt{\frac{4\Gamma_9 - x_9^2 - y_9^2}{\Gamma}} \\ & + y(2\Gamma_9 - x_9^2 - y_9^2) \sqrt{\frac{4\Gamma_9 - x_9^2 - y_9^2}{\Gamma}} \\ & + \frac{1}{\Gamma} y_9(2\Gamma - 3x^2 - 3y^2)(x_9^2 + y_9^2 - 2\Gamma_9) \\ & - y_9(xx_9 + yy_9) \frac{2\Gamma_9 - x_9^2 - y_9^2}{\sqrt{\Gamma(4\Gamma_9 - x_9^2 - y_9^2)}}) \\ \frac{\partial y_9}{\partial t} = & -\frac{3 a^2 \mathcal{G} m m_9}{16 a_9^3 \Gamma_9^2 \varepsilon_9^3} (-2x_9(xx_9 + yy_9) \\ & \times \sqrt{\frac{4\Gamma_9 - x_9^2 - y_9^2}{\Gamma}} + x(2\Gamma_9 - x_9^2 - y_9^2) \\ & \times \sqrt{\frac{4\Gamma_9 - x_9^2 - y_9^2}{\Gamma}} \\ & + \frac{1}{\Gamma} x_9(2\Gamma - 3x^2 - 3y^2)(x_9^2 + y_9^2 - 2\Gamma_9) \\ & - x_9(xx_9 + yy_9) \frac{2\Gamma_9 - x_9^2 - y_9^2}{\sqrt{\Gamma(4\Gamma_9 - x_9^2 - y_9^2)}}). \end{aligned}$$

The evolution of the Sun’s axial tilt is computed in the same manner. The Hamiltonian describing the cumulative effect of the planetary torques exerted onto the solar spin axis is given by Equation (6). Defining scaled Cartesian coordinates

$$\tilde{x} = \sqrt{2\tilde{Z}} \cos(\tilde{z}) \quad \tilde{y} = \sqrt{2\tilde{Z}} \sin(\tilde{z}),$$

we have

$$\tilde{\mathcal{H}} = \sum_j \left( \frac{\mathcal{G} m_j}{4a_j^3} \right) \tilde{a}^2 \left[ \frac{3}{\tilde{\Gamma}} \left( \frac{\tilde{x}^2 + \tilde{y}^2}{2} \right) + \frac{3}{4} \sqrt{\frac{1}{\tilde{\Gamma}\tilde{\Gamma}}} (\tilde{x}x + \tilde{y}y) \right].$$

Accordingly, Hamilton’s equations are evaluated to characterize the dynamics of the Sun’s spin pole, under the influence of

the planets:

$$\frac{d\tilde{x}}{dt} = - \sum_j \left( \frac{Gm_j}{4a_j^3} \right) \tilde{a}^2 \left( \frac{3}{4} y \sqrt{\frac{1}{\Gamma\tilde{\Gamma}}} + \frac{3\tilde{y}}{\tilde{\Gamma}} \right)$$

$$\frac{d\tilde{y}}{dt} = \sum_j \left( \frac{Gm_j}{4a_j^3} \right) \tilde{a}^2 \left( \frac{3}{4} x \sqrt{\frac{1}{\Gamma\tilde{\Gamma}}} + \frac{3\tilde{x}}{\tilde{\Gamma}} \right)$$

Note that unlike  $\Gamma$  and  $\Gamma_0$ , which are conserved,  $\tilde{\Gamma}$  is an explicit function of time, and evolves according to the Skumanich relation. The above set of equations fully specifies the long-term evolution of the dynamical system.

## REFERENCES

- Adams, F. C. 2010, *ARA&A*, **48**, 47
- Albrecht, S., Winn, J. N., Johnson, J. A., et al. 2012, *ApJ*, **757**, 18
- Arnold, V. I. 1963, *Sib. Math. Zh.*, **4**, 2
- Bate, M. R., Lodato, G., & Pringle, J. E. 2010, *MNRAS*, **401**, 1505
- Batygin, K. 2012, *Natur*, **491**, 418
- Batygin, K., & Adams, F. C. 2013, *ApJ*, **778**, 169
- Batygin, K., & Brown, M. E. 2016, *AJ*, **151**, 22
- Batygin, K., Brown, M. E., & Fraser, W. C. 2011a, *ApJ*, **738**, 13
- Batygin, K., Morbidelli, A., & Holman, M. J. 2015, *ApJ*, **799**, 120
- Batygin, K., Morbidelli, A., & Tsiganis, K. 2011b, *A&A*, **533**, A7
- Bayliss, D. D. R., Winn, J. N., Mardling, R. A., & Sackett, P. D. 2010, *ApJL*, **722**, L224
- Brown, M. E., & Batygin, K. 2016, *ApJL*, **824**, L23
- Chandrasekhar, S. 1939, *Introduction to the Theory of Stellar Structure* (Chicago, IL: Univ. Chicago Press)
- Crida, A., & Batygin, K. 2014, *A&A*, **567**, A42
- Fielding, D. B., McKee, C. F., Socrates, A., Cunningham, A. J., & Klein, R. I. 2015, *MNRAS*, **450**, 3306
- Gallet, F., & Bouvier, J. 2013, *A&A*, **556**, A36
- Gomes, R., Deienno, R., & Morbidelli, A. 2016, arXiv:1607.05111
- H  brard, G., Bouchy, F., Pont, F., et al. 2008, *A&A*, **488**, 763
- Heller, C. H. 1993, *ApJ*, **408**, 337
- Henrard, J. 1982, *CeMec*, **27**, 3
- Huber, D., Carter, J. A., Barbieri, M., et al. 2013, *Sci*, **342**, 331
- Izidoro, A., Raymond, S. N., Morbidelli, A., Hersant, F., & Pierens, A. 2015, *ApJL*, **800**, L22
- Jensen, E. L. N., & Akeson, R. 2014, *Natur*, **511**, 567
- Kaib, N. A., & Chambers, J. E. 2016, *MNRAS*, **455**, 3561
- Kaula, W. M. 1962, *AJ*, **67**, 300
- Konigl, A. 1991, *ApJL*, **370**, L39
- Kuiper, G. P. 1951, *PNAS*, **37**, 1
- Lai, D. 2014, *MNRAS*, **440**, 3532
- Lai, D., Foucart, F., & Lin, D. N. C. 2011, *MNRAS*, **412**, 2790
- Laskar, J. 1994, *A&A*, **287**, L9
- Levison, H. F., Morbidelli, A., Tsiganis, K., Nesvorn  y, D., & Gomes, R. 2011, *AJ*, **142**, 152
- Li, G., & Adams, F. C. 2016, *ApJL*, **823**, L3
- Li, G., Naoz, S., Holman, M., & Loeb, A. 2014, *ApJ*, **791**, 86
- Mardling, R. A. 2007, *MNRAS*, **382**, 1768
- Mardling, R. A. 2010, *MNRAS*, **407**, 1048
- McLaughlin, D. B. 1924, *ApJ*, **60**, 22
- Morbidelli, A. 2002, *Modern Celestial Mechanics: Aspects of Solar System Dynamics* (London: Taylor and Francis)
- Morton, T. D., & Winn, J. N. 2014, *ApJ*, **796**, 47
- Murray, C. D., & Dermott, S. F. 1999, *Solar System Dynamics* (Cambridge: Cambridge Univ. Press)
- Narita, N., Sato, B., Hirano, T., & Tamura, M. 2009, *PASJ*, **61**, L35
- Neishtadt, A. I. 1984, *PriMM*, **48**, 197
- Nesvorn  y, D., & Morbidelli, A. 2012, *AJ*, **144**, 117
- Rossiter, R. A. 1924, *ApJ*, **60**, 15
- Souami, D., & Souchay, J. 2012, *A&A*, **543**, A133
- Spalding, C., & Batygin, K. 2014, *ApJ*, **790**, 42
- Spalding, C., & Batygin, K. 2015, *ApJ*, **811**, 82
- Spalding, C., & Batygin, K. 2016, *ApJ*, **830**, 5
- Tremaine, S. 1991, *Icar*, **89**, 85
- Tsiganis, K., Gomes, R., Morbidelli, A., & Levison, H. F. 2005, *Natur*, **435**, 459
- Williams, J. P., Mann, R. K., Di Francesco, J., et al. 2014, *ApJ*, **796**, 120
- Winn, J. N., Fabrycky, D., Albrecht, S., & Johnson, J. A. 2010, *ApJL*, **718**, L145
- Winn, J. N., & Fabrycky, D. C. 2015, *ARA&A*, **53**, 409
- Winn, J. N., Howard, A. W., Johnson, J. A., et al. 2011, *AJ*, **141**, 63
- Winn, J. N., Johnson, J. A., Albrecht, S., et al. 2009, *ApJL*, **703**, L99
- Xiang-Gruess, M., & Papaloizou, J. C. B. 2014, *MNRAS*, **440**, 1179